ELSEVIER

Journal of Alloys and Compounds 253–254 (1997) 121–127

Journal of ALLOYS AND COMPOUNDS

Hydrogen in hard magnetic materials

D. Fruchart[a,*], M. Bacmann[a], P. de Rango[a], O. Isnard[a], S. Liesert[a], S. Miraglia[a], S. Obbade[b], J.-L. Soubeyroux[a], E. Tomey[c], P. Wolfers[a]

[a]*Laboratoire de Cristallographie du C.N.R.S., BP 166, 38042 Grenoble Cedex 9, France*
[b]*Laboratoire de Cristallochimie et Physico-Chimie du Solide, URA CNRS 452, ENSCL, BP 108, 596542 Villeneuve d'Asq Cedex, France*
[c]*ARELEC SA, BP 429 Pau Cedex, France*

Abstract

The rare-earth/transition metal alloys exhibiting high permanent magnet properties are able to reversibly absorb significant amounts of hydrogen. This affects markedly the fundamental characteristics of such intermetallics, and can be used as a probe to understand better the basis of the magnetic interactions. In addition, structural, mechanical and chemical aspects of the hydrogenation process are used to improve the synthesis of appropriate powders for the magnet technologies.

Keywords: Magnets; HDDR; Hydrogenation

1. Introduction

Modern hard magnetic materials are based on R–T couples of rare earth and transition metals. Combination of these elements in alloys or in interstitial stabilised intermetallics (B, C, N, Si...) allows maximisation of intrinsic and extrinsic properties such as:

a high degree of magnetisation and a high T atom density; then a large induction is obtained from an anisotropic magnet,
a high magnetocrystalline anisotropy from the major contribution of the R crystal electric field; consequently a large coercivity can be developed from an appropriate microstructure.

Dense intermetallic systems exhibit mostly octahedral and tetrahedral interstitial sites, attractive for hydrogen atoms if neighboured by R, the electropositive elements. Stable and reversible hydrides can be synthesised, exhibiting medium or weak hydrogen uptakes. However, the structural and physical properties of these materials are, most of the time, affected markedly upon hydrogenation.

This paper is divided in two parts with firstly, a review of the fundamental aspects of the behaviour of the metal hydrides, and secondly, a review of the uses of hydrogen as a metallurgy agent for the fine powder technologies, hydrogen decrepitation (HD) and (HDDR) hydrogenation, disproportionation, desorption, recombination.

2. Characteristics of the performance of hard magnetic materials

2.1. General principles

In the early 70's, very high anisotropy levels were achieved with the series $SmCo_5$ and their derivatives Sm_2Co_{17} [1]. They were found to combine several important properties such as the samarium crystal field characteristics in uniaxial type of structures and a high level of magnetisation due to the large cobalt density, such a magnetisation persisting at high temperatures. The search for better performance materials, higher level of magnetisation, lower cost particularly with regards to the expensive cobalt,... was satisfied at the end of 1983 with the discovery of the new series of ternary borides of formula $R_2Fe_{14}B$ [2,3]. Hydrogen has been demonstrated to react with these borides, to increase (more particularly) the rather low Curie temperature of the intermetallics. Then, such a trend was shown to occur as well in the iron rich alloys, with formula R_2Fe_{17} and $RFe_{12-x}M_x$, which were revealed to form ternary hydrides.

So, we will examine most of the important properties of

*Corresponding author.

0925-8388/97/$17.00
PII S0925-8388(96)03063-0

the alloys and their potential as magnets, and the technological routes used for making appropriate powders.

2.2. Fundamentals of the R–T metal magnets

Since transition metals can ensure a much larger magnetic density in close packed alloys, it is achieved with the ferromagnetic coupled elements Fe and Co which have magnetic moments of about 2.2 and 1.7 μ_B, respectively. For that, the first element is to be preferred, but unlike cobalt which exhibits a strong ferromagnetic character, the magnetic moments as the Fe–Fe magnetic interactions, are found to be very sensitive to the coordination and metal–metal distance. So for Fe-rich alloys, there is a balance between a high moment density and the variable exchange forces. In any case, the contributions from the R–T and R–R exchange interactions to the Curie temperature are at most, 5 to 10 times lower than that of a pure 3d origin. For these reasons and due to the cost, the R proportion must be rather limited. The R–T exchange couplings lead to ferromagnetic and ferrimagnetic arrangement respectively (due to the spin orbit couplings $J=L\pm S$) when alloying light or heavy rare earth metals respectively, the first series only being practically acceptable. In all the cases, the interatomic exchange interactions have a metal character, i.e. via the conduction electron density, or of RKKY type. An axial crystal structure is needed in order to favour an axial spin vector character, i.e. an anisotropic inductive material. Thus, high or low R site symmetries can exist, and in the latter case, the high order crystal electric field (CEF) terms should be non negligible. Consequently from their thermal behaviour and that of the exchange terms, spin reorientation transitions (SRT) are expected. Recently, the dominant CEF terms have been proved to be, not only of point charge model origin, but a comparable contribution of the valence electron concentration (VEC) has to be accounted for [4].

Permanent magnets can be developed when these properties are maximised and then, via a well built microstructure, to produce suitable extrinsic characteristics. Firstly, the particles must be textured in such a way that the individual crystallites are all directed along a common axis in the bulk magnet. Secondly, the microstructure has to be made coercive, via mechanisms involving either pinning the domain wall, or inhibiting the development of reverse domains. A high energy product $(BH)_{max}$ that is the signature of the stored magnetic energy in the magnet can be reached via H-metallurgy processes at the micrometric scale.

3. Types of hard magnetic metal materials

3.1. The $SmCo_5$ type of magnets

The crystal structure is an isotype of the famous H-storage series $LaNi_5$. In the hexagonal $P6/mmm$ space group, the insertion sites are related to both octahedral and tetrahedral metal coordinations [5]. It has been seen experimentally that the cobalt-containing compounds accommodate up to 3.5 H/fu only, compared with that of $LaNi_5$ which is more than 6 H/fu (Fig. 1).

3.2. The Sm_2Co_{17} type of magnets

There are three well defined derivatives of the previous type of formula that are the R-Th_2Zn_{17}-type (R-3m), H-Th_2Ni_{17}-type ($P6_3/mmc$) and $TbCu_{8.5}$-type ($P6/mmm$). They differ by the scheme of the substitution of one rare earth atom by a pair of T metals (called dumbbell), giving rise to different types of structures (Fig. 1). In fact a magnet of so-called R_2Co_{17} type is coercive assembly of a major 2–17 phase and minor ones such as 1–5 and related 1–3 types [6]. For such an equilibrium, additional transition metals are alloyed (Zr, Cu, Fe...), giving rise to a complex phase diagram.

3.3. The R-Fe-B series

Nowadays, these materials are the most applied hard metal magnets, and the market is growing markedly. The tetragonal structure of the majority phase of $R_2Fe_{14}B$ formula ($P4_2/mnm$) can be decomposed schematically in an iron-rich σ-type of slabs, alternating with R and B-containing (001)-planes (Fig. 2). A limit of 5.5 H/fu has

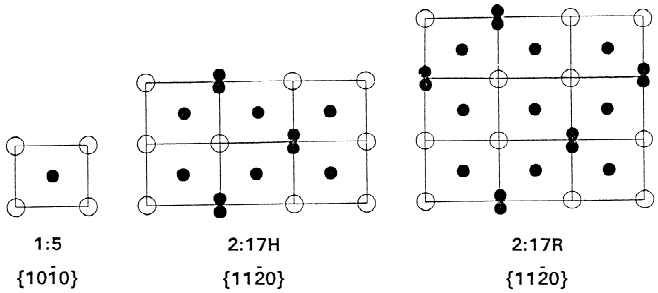

Fig. 1. Schematic crystal structure of $SmCo_5$ and of the R_2Fe_{17} types of compounds. In the $TbCu_{8.5}$ type, T dumbbells (black double dots) are randomly distributed on the R sites (white dots). The planes containing Co only (black dots), are represented, the normal Co atoms in R-plane are not.

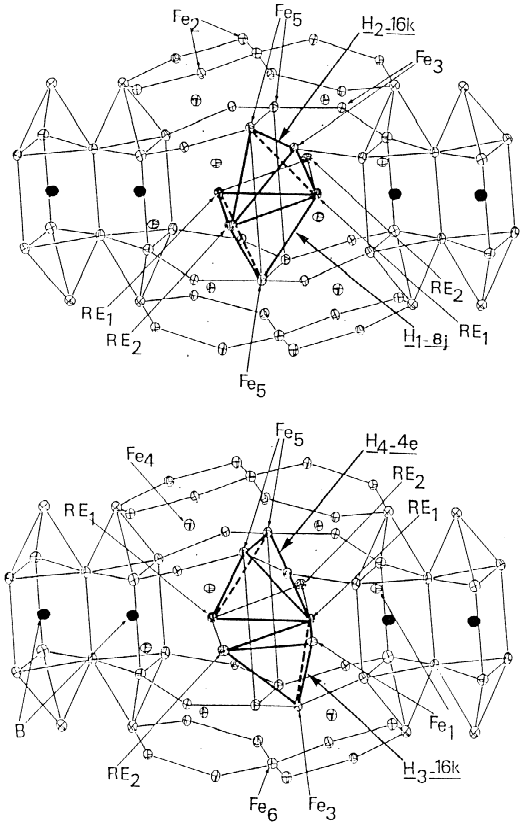

Fig. 2. Part of the crystal structure of $R_2Fe_{14}BH_x$ with the H-attractive tetrahedra.

been determined with the filling of tetrahedral interstitial sites [7].

3.4. The R_2Fe_{17} and $R_2Fe_{17}X_x$ compounds (X=H, C, N)

Demonstration of a favourable magnetovolume effect induced upon hydrogen insertion [8] has lead to the further discovery of promising magnets, Sm_2Fe_{17} carbides and nitrides [9,10]. In the case of the ternary hydrides, a maximum of 5 H/fu has been found to be accommodated by the rhombohedral or the hexagonal types of structures described in Part III-2 (Fig. 3).

3.5. The 'R-Fe_{12}' type of compounds

A limited series of non magnetic T elements are required in a rather small amount to stabilise the tetragonal *I*4/*mmm* type of compounds [11]. Hence, the Curie temperature is directly dependent upon the amount of alloyed iron [12]. Once again, this type of material is directly dependent upon the amount of alloyed iron [12]. Once again, this type of material is directly derived from the $SmCo_5$ type structure via a specific R to Fe–Fe dumbbell substitution [11] (Fig. 4). The H-attractive site has an octahedral coordination and corresponds to 1 H/fu.

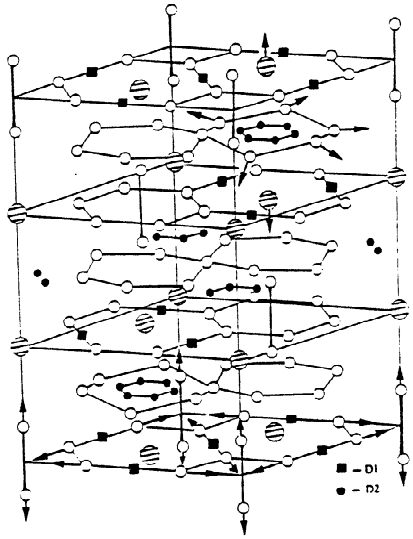

Fig. 3. Crystal structure of the ternary $R_2Fe_{17}H_5$ (R-3*m*). The arrows show the metal atom displacements induced by hydrogen insertion.

Recently, other H-attractive sites have been proved to exist [13].

4. Chemical and physical aspects upon hydrogenation of R–T magnet materials

4.1. Phase diagrams

Except for the $SmCo_5$ type of materials, no clear plateau pressure can be observed in the R–T metal hydrogen phase diagrams. Most of the time, the equilibrium isotherms look like the behaviours of solid solutions (Fig. 5). In the less R-rich series of materials (R_2T_{17}, $R_2Fe_{14}B$, RT_{12}), hydrogen is more particularly condensed in the R-dense parts of the structure. Consequently, the elastic atomic interactions appear more and more smoothed with increase of *R*/*T* ratio.

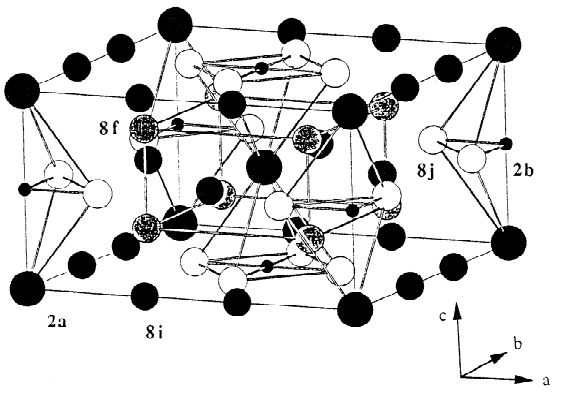

Fig. 4. Crystal structure of $RF_{10.5}Mo_{1.5}H_1$. Hydrogen occupies the 2b octahedral site up to 1 H/fu.

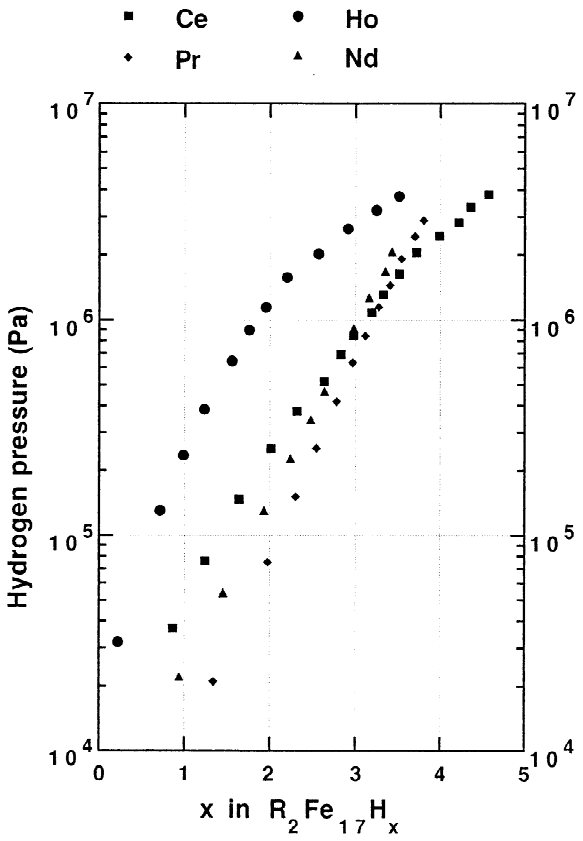

Fig. 5. Isotherm equilibrium at room temperature for some $R_2Fe_{17}H_x$ compounds.

4.2. Physical properties

4.2.1. $SmCo_5$

In SmCo5, a change of magnetisation occurs with the hydrogen insertion, this concerns the cobalt lattice [14], (as for most of the R-Co alloys) where a marked reduction of the magnetic Co moment occurs. However, the local moment of this series of materials is highly sensitive either to the chemical bond or to the application of high magnetic fields. Some complete depolarisation effects have been observed upon hydrogenation [14]. Yamaguchi et al. have pointed out a direct relationship between the magnetic entropy controlled by the application of an external field on the $SmCo_5H_x$ system and the enthalpy of formation of different metal-hydrides (β to γ phase transformation). Studies have been undertaken both in the gas–metal and in electrochemical modes [15].

4.2.2. R_2T_{17} types of hydrides, T=Fe, Co

Typically the isotherms recorded on these systems correspond to solid solution like behaviour. Hydrogen has been found to occupy two types of interstitial site, an octahedral site with a maximum of 3 H/fu (2R–4T) and a tetrahedral one with a maximum of 2 H/fu. Limitation at 1/3 of the theoretical possibilities of the latter site is according to the Switendick-Westlake criteria for occupation of next neighbour interstitial sites [16]. Neutron diffraction investigations have confirmed this limitation, and clearly show that the octahedral sites are by far the most attractive sites [17]. A systematic analysis versus the hydrogen content shows that the different site occupation correspond to well defined cell parameter expansions (Fig. 6).

Unlike cobalt, iron is a weak ferromagnet element, and in alloys, namely, those related to the tetrahedral close packed structures, short T–T distances are observed (e.g. dumbbell distance is less than 2.4 Å compared to 2.5 Å in α-Fe). The strength of the Fe–Fe magnetic exchange interactions are strongly dependant on the orbital overlap i.e. the interatomic distance. As hydrogen expands the cell volume and local distances in the R_2Fe_{17} series, it leads to a dramatic increase in the Curie temperature by about 150 to 200 K [17]. It can be justified by reference to the Slater-Néel curve, if one considers a negative to positive change of critical exchange interactions.

Less effective but systematic is the increase in magnetisation related to an increase in the local magnetic moments only (by 5 to 10%). Opposite but coherent with the hydrogen induced cell expansion are the results obtained under an external pressure. A scale factor of 1 GPa/H can be deduced from the comparison of these two cell volumes and Curie temperature behaviours. A general analysis in terms of magnetoelastic effects upon hydrogenation appears to be consistent with a localised picture of magnetics instead of an itinerant one [18].

Magnetisation measurements, systematically performed on oriented powders before and after hydrogenation, reveal a net increase in the saturation facilities for intermediate applied magnetic fields. A local type approach has been undertaken on the $Gd_2Fe_{17}H_x$ system by means of the ^{169}Gd Mössbauer spectroscopy. The A_2^0 second order CEF parameter has been shown to markedly decrease and vanish upon hydrogenation [17]. The magnetocrystalline anisotropy of R origin is deeply depressed when the R_2T_{17}

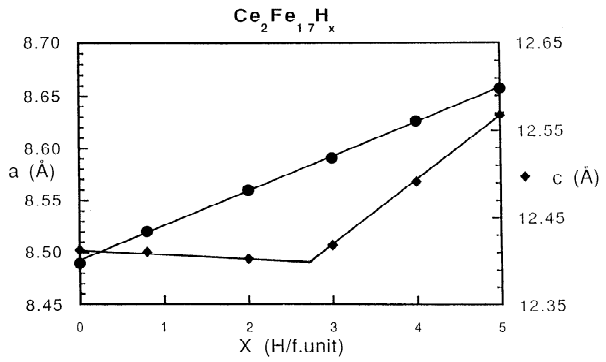

Fig. 6. Cell parameter behaviours with x of $Ce_2Fe_{17}H_x$.

when the R_2T_{17} alloys are hydrogenated, it is the reverse of that which occurs in the parent carbides and nitrides [9,10].

4.2.3. The $R_2Fe_{14}BH_x$ systems

These compounds have been studied more extensively owing to the fundamental interest of a new series of ternary borides, and to the large domain of applications. Once more the PCT measurements reveal a solid solution like behaviour, neutron diffraction investigations (R=Y, Ce, Nd, Ho, Er) indicated a coherent scheme of occupancy for the four sites involved in the hydrogen absorption [7,13,17,19] (Fig. 2), depending on the alloyed R-element (light and large to heavy and small rare earth atom) the relative occupancy of the most attractive types of sites (R_3Fe and R_2Fe_2) reveal differences during the first step of hydrogenation. A clear anisotropic cell expansion results from the selectivity of the site under filling with the hydrogen content. Since Fe neighbours are at some very short Fe–Fe distances (Fe3–Fe5, Fe5–Fe5), once more a large increase in Curie temperature results in the increase of these critical distances (Fig. 7). However the T_c increase is markedly dependant on the filling scheme of the sites (depending on the size of the rare earth atom).

A systematic but relatively smaller increase in magnetisation is observed, when compared to that observed upon hydrogenation of the 2–17 series. Here again a reduction of the band width of Fe with the increase of volume is expected, and is relevant with the weak ferromagnetic character of this element. A review paper on the relationship between the Wigner-Seitz volume and the local moment of Fe in intermetallics experimentally supports this point of view [20].

Finally, a dramatic decrease of the magnetic anisotropy parameters is observed. As for the exchange forces, the decrease is faster when the most attractive tetrahedral sites are filled, which are also the R-richest ones. The CEF parameters are concerned in such a way that existing SRT (e.g. R=Nd, Ho, Er, Tm) are changed continuously, monitored by the hydrogen uptake. A unique set of critical exponents well applies to the variations of the CEF upon H insertion [21]. These changes of the parameters can be understood in terms of the contribution to CEF of the valence electron distribution [4].

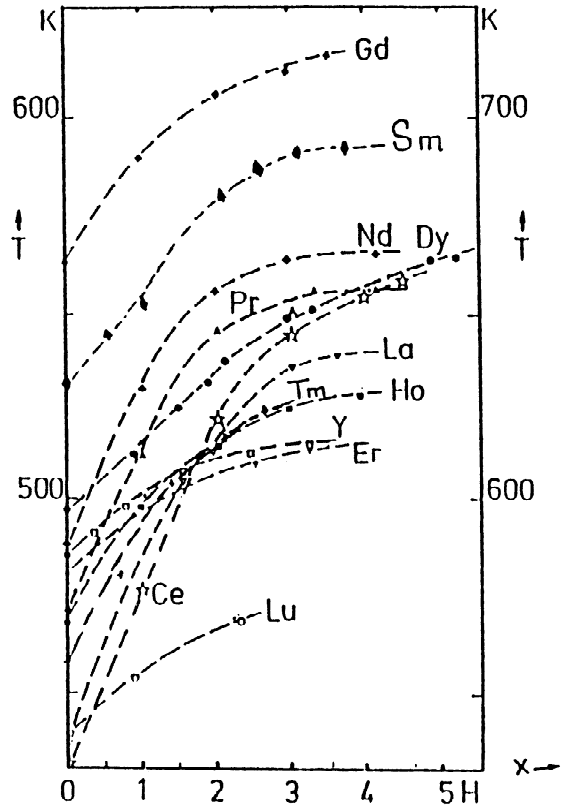

Fig. 7. Curie temperature behaviour with x of $R_2Fe_{14}BH_x$.

4.2.4. The $RFe_{12-x}M_x$ series

First, hydrogen was observed to fill unique R_2Fe_4 octahedral sites (2b position), that correspond to one of the existing sites in the parent RCo_5 and R_2Fe_{17} structures. A total occupation of this site corresponds to 1 H/fu. However, it has been proved recently that when charged with more hydrogen [13,22,23], a triangular bi-pyramidal site is a second insertion site if electro-attractive elements are substituted to Fe (Ti>V>Mo...) [24].

Neutron diffraction shows that hydrogen insertion leads only to limited increases in the Fe–Fe critical distances (2.39 Å). However, the Curie temperature of the series is increased by about 11% upon hydrogenation. As the mean increase in bulk magnetisation is only 3–4%, this does not explain the larger increase of magnetic moment observed by neutron diffraction [13,25]. A negative electron conduction polarisation should compensate the change in localised moment. Band structure calculations reveal a compensation contribution mainly from the non magnetic atom (e.g. Mo...) [26].

In this series the most unexpected trend appears to be the net reinforcement of both the CEF (R) and 3d (Fe) magnetocrystalline anisotropy terms in the hydrogenated compounds in comparison with the alloys [13,25]. When H is inserted in the 2b sites, the A_2^0 CEF parameter increases and both the axial character ($\alpha_J>0$ type of R elements) and the planar character ($\alpha_J>0$ type of R elements) are reinforced. It is exactly what happens with the parent carbides and nitrides for the reverse signs of the second order Stevens' terms. Hence, the spatial distribution of the valence electron density reference to the [001]-axis is of prime importance on the behaviour of the magnetocrystalline anisotropy terms in the 1–12 series. $SmFe_{11}MoH$ has more anisotropic characteristics than the parent nitride $NdFe_{11}MoN$ [25].

5. Hydrogen and microstructure for magnets

5.1. Properties and mechanisms

The coercive forces that make the bulk magnet resistant to depolarisation are either related to a wall pinning mechanism, or correspond to the potential nucleation of reverse domains. In both cases the microstructure in terms of grains and crystallites (size, shape, inclusion, surface, intergranular phase...), is of prime importance [6]. If the 2–17 type of magnets belong to the pinning type as for the melt spun 2–14–1 type, the sintered $Nd_{15}Fe_{77}B_8$ type magnets follow the second mechanism. In any case the size of the elementary crystallites and that of the free particles must be controlled as well as the composition and repartition of the minor intergranular phases, to avoid the propagation of the wall domains in the bulk. Furthermore, if the grains are textured i.e. the crystallites being essentially oriented along a common direction, the resulting magnet gains inductive force by a factor 2 compared with that of the isotropic situation. In order to develop or to preserve the optimised qualities of a coercive and anisotropic microstructure, often mechanical crushing is not the best route. Moreover, such a technique is expensive in machines and time. Hydrogenation has proved to be suitable for the H-attractive alloys, and two routes can be used for: HD that is hydrogen decrepitation [27], mainly intergranular or intragranular [28], and HDDR that consists in disproportionation of the starting alloys and recombination to form an improved microstructure after desorption of the R-hydrides [29]. The challenge of anisotropic and coercive powders of high performance materials corresponds to the larger and larger needs in bonded magnets.

5.2. The HDDR route

It was first reported by Takeshita et al. [29], but also actively studied by Harris et al. [28]. A scheme of principle of the operating conditions is give in [29] and the chemical equation is give in [30], starting from non-stoichiometric material (without initial coercivity or anisotropy). Large coercive forces have been obtained from well controlled homogeneous microstructures developed after dehydrogenation and recombination. Typically the resulting magnets are isotropic, but an oriented growth of the elementary crystallites from textured precursors or via epitaxy mechanisms due to elemental additives (Zr, Nb...) can induce a certain level of texture [28], similarly texture can be developed during recrystallisation under high magnetic fields [30]. Fig. 8 shows hysteresis cycles recorded on HDDR-treated $R_2Fe_{14}B$-type of powders for magnets. The HDDR technique is also used as one of the first treatments of the microstructure of the Sm_2Fe_{17} alloys prior to nitrogenation [31].

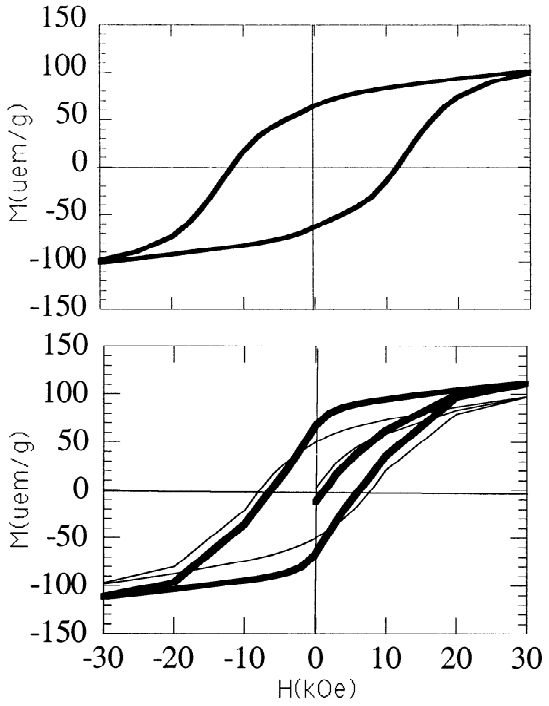

Fig. 8. Magnetisation cycles of HDDR processed $Nd_2Fe_{14}B$ types of powders (up: isotropic, down: anisotropic).

5.3. The HD route

The low temperature hydrogenation treatment is schematised in [28], and it was first proposed to supersede the mechanical crushing required in the powder metallurgy process for making sintered magnets. Since, from coercive and textured massive precursors, these main characteristics have been restored at a high level in free powders after dehydrogenation and subsequent heat treatments [32], an alternative way for producing anisotropic bonded magnets was opened. Fig. 9 shows a hysteresis cycle recorded on a HD-treated $R_2Fe_{14}B$-based powder (nucleation-type coer-

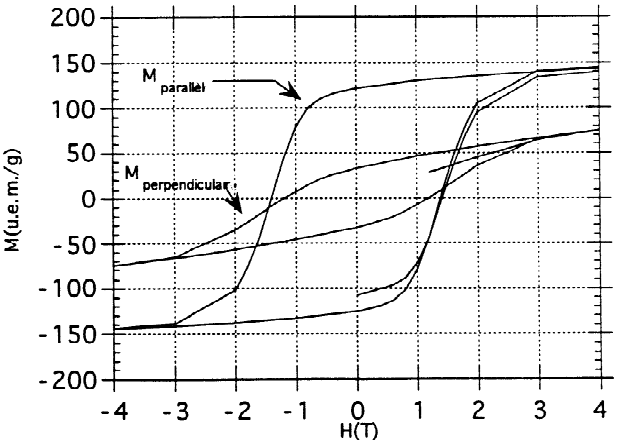

Fig. 9. Magnetisation cycle of a HD processed $Nd_2Fe_{14}B$ type of anisotropic powder.

civity). The HD route was shown to be well suited for powders of cobalt-rich 2–17 alloys (pinning-type coercivity) [33].

6. Conclusion

It was observed that hydrogen insertion in hard metal magnets of R–T type, induces marked changes in the fundamental properties of these materials. Curie temperatures of the iron-rich compounds increases dramatically as opposed to the magnetocrystalline anisotropy of the R element (except in the RM_{12} type of alloys), which drops steeply. The magnetisation of the weak ferromagnet iron is raised by 5 to 10%. All these phenomena are now well understood in terms of a more localised rather than an itinerant picture. Hydrogen can be used as a probing element of these fundamental properties.

Hydrogenation in terms of mechanical effects has been used (profitably) in technical processes involving the development of coercive and anisotropic powders required for the technology of high performance bonded magnets.

References

[1] K.J. Strnat, W. Ostertag, N.J. Adams and J.C. Olson, *5th Rare Earth Research Conf.*, Ames, Iowa, 1965.
[2] M.M. Sagawa, S. Fujirama, M. Togawa, H. Yamamoto and Y. Matsuura, *J. Appl. Phys., 55* (1984) 2083.
[3] J.J. Croat, J.F. Herbst, R.W. Lee and F.E. Pinkerton, *J. Appl. Phys., 55* (1984) 2078.
[4] R. Coehoorn, in G.J. Long and F. Grandjean (eds.), *Supermagnets, Hard Magnetic Materials*, Kluwer Academic Publishers, Dordrecht (1991) 133.
[5] C. Lartigue, *P. and M. Thesis*, Curie University, Paris, 1984.
[6] K.J. Strnat, in E.P. Wolfarth and K.H.J. Buschow (eds.), *Ferromagnetic Materials*, Vol. 4, Elsevier, 1988, p. 131.
[7] D. Fruchart, P. Wolfers, P. Vuillet, A. Youanc, R. Fruchart and P. l'Heritier, in I.V. Mitchell (ed.), *Nd-Fe Permanents Magnets. Their present and future applications*, C.E.C. Bruxelles, 1984.
[8] W.X. Zhong, K. Donnelly, J.M.D. Coey, B. Chevallier, J. Etourneau and T. Berlureau, *J. Mat. Science, 23* (1988) 329.
[9] X.P. Zhong, R.J. Radwanski, F.R. de Boer, T.H. Jacobs and K.H.J. Buschow, *J. Magn. Magn. Mat., 86* (1990) 333.
[10] J.M.D. Coy and H. Sun, *J. Magn. Mat., 87* (1990) L251.
[11] J.V. Florio, R.E. Rundle and I.A. Snow, *Acta Cryst., 5* (1952) 449.
[12] K.H.J. Buschow and D.B. de Mooij, in I.V. Mitchell (ed.), *Concerted European Action on Magnets*, Elsevier, 1989, p. 63.
[13] S. Obbade, *Thesis, J.* Fourier University, Grenoble, 1991.
[14] K.H.J. Buschow, in K.A. Gschneider and L.R. Eyring (eds.), *Handbook on the Physics and Chemistry of Rare-Earths*, Vol. 6, North Holland, 1984.
[15] I. Yamamoto, M. Yamaguchi, T. Goto and S. Miuara, *J. Less Comm. Metals, 172* (1991) 79.
[16] D.G. Weslake, *J. of the Less-Comm. Met., 90* (1983) 251.
[17] O. Isnard, *Thesis, J.* Fourier University, Grenoble, 1992.
[18] D. Fruchart, O. Isnard, S. Miraglia and J-L. Soubeyroux, *J. Alloys Comp., 231* (1995) 18.
[19] P. Dalmas de Reotier, D. Fruchart, L. Pontonnier, F. Vaillant, P. Wolfers, A. Yaouanc, J.M.D. Coey, R. Fruchart and P. L'Heritier, *J. Less-Comm. Met., 129* (1987) 133.
[20] O. Isnard and D. Fruchart, *J. Alloys Comp., 205* (1994) 1.
[21] M.D. Kuz'min, L.M. Garcia, I. Plaza, J. Bartolomé, D. Fruchart and K.H.J. Buschow, *J. Magn. Magn. Mat., 145* (1995) 239.
[22] L.Y. Zhang, S.G. Sankar, W.E. Wallace and S.K. Malik, *6th Intern. Symp. on Magn. Anis. and Coerc.* in *Rare Earth-Transition Met. Alloys*, Pittsburgh, USA, 1990, p. 493.
[23] R. Bezdushinyi, R. Damianova, N. Stanev and A. Apostolov, *J. Magn. Magn. Mat.,* (1996) in press.
[24] D. Fruchart, M. Bououdina, S. Miraglia, J.L. Soubeyroux and S. Obbade, *J. Alloys Comp., 253–254* (1997) 298–301.
[25] E. Tomey, *Thesis, J.* Fourier University, Grenoble, 1994.
[26] R. Lorenz, J. Hafner, S.S. Jaswal and D.J. Sellmeyer, *Phys. Rev. Letts., 74, 18* (1994) 3688.
[27] D. Fruchart, S. Miraglia, L. Pontonnier, P. de Rango, J.-L. Soubeyroux, R. Fruchart, P. Mollard and R. Perrier de la Bâthie, *Proc. the 12th Intern. Workshop on Rare-Earth Magnets and their Applications*, Birmingham, U.K., 1991, 511, and references herein.
[28] I.R. Harris, *Proc. the 11th Workshop on Rare-Earth Magnets and their Applications*, Canberra, Australia, 1993, 347, and references herein.
[29] T. Takeshita and R. Nakayama, *Proc. 10th Intern. Workshop on Rare-Earth Magnets and their Applications*, Kyoto, Japan, 1989, and references herein.
[30] S. Liesert, P. de Rango, J.-L. Soubeyroux, D. Fruchart and R. Perrier de la Bâthie, *J. Magn. Magn. Mat. 7023* (1996).
[31] R. Arlot, P. de Rango, D. Fruchart, J.-L. Soubeyroux and R. Perrier de la Bâthie, *Proc. the 14th Intern. Workshop on Rare-Earth Magnets and their Applications*, Sao Paulo, Brazil, 1996, in press.
[32] D. Fruchart, S. Miraglia, R. Perrier de la Bâthie, R. Fruchart and P. Mollard, Patent EP 90 06-206.
[33] O. Isnard, S. Miraglia, D. Fruchart, D. Boursier and P. l'Héritier, *J. Magn. Magn. Mat., 103* (1990) 157.